AIP Applied Physics Letters

Spectral analysis of thermal boundary conductance across solid/classical liquid interfaces: A molecular dynamics study

Ashutosh Giri and Patrick E. Hopkins

Citation: Applied Physics Letters **105**, 033106 (2014); doi: 10.1063/1.4891332
View online: http://dx.doi.org/10.1063/1.4891332
View Table of Contents: http://scitation.aip.org/content/aip/journal/apl/105/3?ver=pdfcov
Published by the AIP Publishing

Articles you may be interested in
Analytical model for the effects of wetting on thermal boundary conductance across solid/classical liquid interfaces
J. Chem. Phys. **140**, 154701 (2014); 10.1063/1.4870778

Pressure dependency of thermal boundary conductance of carbon nanotube/silicon interface: A molecular dynamics study
J. Appl. Phys. **112**, 053501 (2012); 10.1063/1.4749798

Role of wetting and nanoscale roughness on thermal conductance at liquid-solid interface
Appl. Phys. Lett. **99**, 073112 (2011); 10.1063/1.3626850

Heat conduction across a solid-solid interface: Understanding nanoscale interfacial effects on thermal resistance
Appl. Phys. Lett. **99**, 013116 (2011); 10.1063/1.3607477

Molecular dynamics simulations of thermal resistance at the liquid-solid interface
J. Chem. Phys. **129**, 174701 (2008); 10.1063/1.3001926

AIP Journal of Applied Physics

Journal of Applied Physics is pleased to announce André Anders as its new Editor-in-Chief

This article is copyrighted as indicated in the article. Reuse of AIP content is subject to the terms at: http://scitation.aip.org/termsconditions. Downloaded to IP: 137.54.21.74 On: Tue, 22 Jul 2014 15:57:16

APPLIED PHYSICS LETTERS 105, 033106 (2014)

Spectral analysis of thermal boundary conductance across solid/classical liquid interfaces: A molecular dynamics study

Ashutosh Giri[a] and Patrick E. Hopkins[b]
Department of Mechanical and Aerospace Engineering, University of Virginia, Charlottesville, Virginia 22904, USA

(Received 6 May 2014; accepted 14 July 2014; published online 22 July 2014)

We investigate the fundamental mechanisms driving thermal transport across solid/classical-liquid interfaces via non-equilibrium molecular dynamics simulations. We show that the increase in thermal boundary conductance across strongly bonded solid/liquid interfaces compared to weakly bonded interfaces is due to increased coupling of low-frequency modes when the solid is better wetted by the liquid. Local phonon density of states and spectral temperature calculations confirm this finding. Specifically, we show that highly wetted solids couple low frequency phonon energies more efficiently, where the interface of a poorly wetted solid acts like free surfaces. The spectral temperature calculations provide further evidence of low frequency phonon mode coupling under non equilibrium conditions. These results quantitatively explain the influence of wetting on thermal boundary conductance across solid/liquid interfaces. © *2014 AIP Publishing LLC*.
[http://dx.doi.org/10.1063/1.4891332]

In nanosystems and devices, resistance to thermal transport is mostly limited by the interface.[1–3] As device dimensions shrink to the sub-micron length scale, heat dissipation plays an important role in their reliability and performance. Recently, properties of solid/liquid interfaces have been shown to be significant in designing nanoscale systems and also in understanding various biological and chemical processes.[4–7] Even though the first quantitative measurement of thermal boundary conductance (TBC), h_K, was reported between Cu and liquid He (Ref. 8), the vibrational TBC between solid/classical-liquid interfaces has received significantly less attention compared to their solid/solid counterparts. Not only has the fundamental physics driving energy transport across solid/solid interfaces been extensively studied compared to the solid/liquid interfaces but also the influence of surface roughness, impurities, and bonding at solid/solid interfaces have also been well established with numerous experimental investigations (for a detailed review of the topic, the reader is referred to Ref. 2, and the references therein). Along these lines, experimental measurements of TBC across planar solid/classical-liquid interfaces are limited due to complications introduced by the low thermal conductivities (large thermal resistivities) of liquids, making it difficult to separate the resistance due to the interface from that of the resistance due to the two layers.[9–11]

In recent years, molecular dynamics (MD) has proven as an alternative to advance understanding beyond experimental measurements of the Kapitza resistance across solid/classical-liquid interfaces. Barrat and Chiaruttini[12] used MD simulations to show that the solid/liquid thermal boundary conductance increases with an increase in the wetting of a surface; Xue *et al.*[13] showed the same dependence with their MD simulations and also highlighted that the Kapitza resistance exhibits a power law dependence for highly wetting fluids. Shenogina *et al.*[14] took this a step further by tuning the adhesion energy at the interface through surface topology modifications with self assembled monolayers. They showed excellent agreement with the experimental findings by Ge *et al.*[10] for similar systems. Improving on these results even further, Acharya *et al.*[15] demonstrated that h_K at solid/liquid interfaces is also influenced by the chemical heterogeneity, roughness, and contact area. Issa and Mohamad[16] also studied structural modification of the solid surface but through geometrical nanopatterning which was shown to affect the vibrational coupling of the adsorbed liquid and the solid surface. Furthermore, the liquid molecular structure formed near the solid surface has been shown to dominate the interfacial phonon transport at cold surfaces (as opposed to the hotter side), where the liquid density was observed to be higher.[17–20] Solidifying these works, Kim *et al.*[17] proposed that the temperature jump at the boundary is a function of the wettability, the relative thermal oscillation of the solid and the liquid, the wall temperature, and the local thermal gradient.

All of the aforementioned works allude to the fact that the variation in the local phonon density of states (DOS) can explain the different thermal responses of variably wetted interfaces. The current theoretical understanding of the TBC across solid/liquid interfaces are based on continuum theories such as the acoustic mismatch model and the diffuse mismatch model.[21] However, these theories cannot correctly predict the results from recent experimental and computational works. This deviation is due to the fact that these theories consider bulk properties of the materials and ignore the surface wettability and the nanoscale structure when predicting the interface conductance.

Recently, we developed an analytical model to predict the TBC across solid/liquid interfaces, which takes into account how wetting influences heat flow across the interfaces.[22] Our model is partly based on previous works which have established that wetting at a solid/liquid interface

[a]Electronic mail: ag4ar@virginia.edu
[b]Electronic mail: phopkins@virginia.edu

 © 2014 AIP Publishing LLC

This article is copyrighted as indicated in the article. Reuse of AIP content is subject to the terms at: http://scitation.aip.org/termsconditions. Downloaded to IP: 137.54.21.74 On: Tue, 22 Jul 2014 15:57:16

dictates the shear oscillations in the liquid layer close to the interface. It has been well established that size effects render the no-slip boundary condition inapplicable at the micron and sub-micron length scales, and that slip lengths of the liquid molecules are highly dependent on the wetting properties and surface roughnesses.[23–27] Therefore, by infusing the diffuse mismatch theory with recent developments on phonon theory of liquid thermodynamics,[28–30] we proposed a model to predict h_K for varying degrees of hydrophilic and hydrophobic surfaces.[22] Our model was based on the hypothesis that the TBC dependence on wetting is due to the variation in low frequency phonon mode coupling across the interface, which is dependent on the interfacial bond.

In this work, we use nonequilibrium MD (NEMD) simulations to study the atomistic mechanisms and vibrational physics behind thermal transport across variably wetted interfaces. We find that the variable interfacial bonding environment characterizing solid/classical liquid interfaces with different wetting conditions has the most pronounced effect on the coupling of low frequency modes, which supports our previous theoretically driven hypothesis.[22] We analyze the local phonon DOS of the solid monolayer of atoms immediately adjacent to the interface and quantify that the thermal transport dependence on wetting is primarily due to varying strengths of transverse mode coupling through the interface. We hypothesize that for strongly wetted interfaces, the zero slip boundary condition applies, where the velocity of the liquid phonon modes near the interface assume those of the transverse modes in the solid. We calculate the spectral temperature for variably bonded solid/liquid interfaces when a temperature gradient is imposed, which we use as a metric to quantify the strength of interfacial phonon coupling. We conclude that the fundamental mechanism behind the influence of interfacial bond strength on Kapitza conductance at solid/liquid interfaces is the coupling of the low frequency vibrations. We note this is similar to the mechanisms that we have previously observed for phonon coupling at variably bonded solid/solid interfaces using NEMD.

Our molecular dynamic simulations employ the 6–12 Lennard-Jones (LJ) potential, $U(r) = 4\varepsilon[(\sigma/r)^{12} - (\sigma/r)^{6}]$, where U is the interatomic potential, r is the interatomic separation, and σ and ε are the LJ length and energy parameters, respectively. As we are interested in the general interactions contributing to thermal transport as opposed to specific properties of materials, the LJ system will be sufficient to provide the necessary qualitative insight on thermal transport. For simplicity, argon was chosen to parameterize the LJ potential with $\sigma = 3.045$ Å and the lattice constant $a_0 = 1.56\sigma$.[31] The radius beyond which the potential was truncated was set to $r = 2.5\sigma$. The energy parameter for the LJ solid atoms is prescribed to be $\varepsilon_{\text{s-s}} = 0.103$ eV, while the energy parameter for liquid atoms is set as $\varepsilon_{\text{l-l}} = 0.0103$ eV. These choices ensure that the liquid atoms melt, whereas the solid atoms hold their crystallographic configuration; the melting point of the LJ solid is proportional to the energy parameter defining the solid-solid interaction and is approximately equal to $\varepsilon_{\text{s-s}}/2k_B$.[32] All atomic masses are set to 40 a.m.u. and the interaction strengths between the solid and liquid atoms are in the range 0.0052–0.103 eV.

The simulation cell is 58 a_0 in the z-direction and 10 a_0 in the x- and y-directions; the geometry is shown in the top panel of Fig. 1. Periodic boundary conditions are applied in all three directions. The atoms are initially placed in an fcc crystal orientation and allowed to equilibrate at a predefined temperature of 170 K. The equilibration is performed for a total of 1×10^6 time steps with a time step of 0.5 fs under the Nose-Hoover thermostat.[33] The reverse NEMD method is applied to create a steady heat flux in the system and the resulting temperature gradient is calculated along the direction of the heat flux. The details of the reverse NEMD process are described in Ref. 34. The heat flux is calculated as $q = \Delta E/2A\Delta t$, where A is the surface area perpendicular to the heat flux, Δt is the time step, and ΔE is the kinetic energy swapped between the hot and the cold slab at each time step. Note, increasing the simulation cell size did not change the h_K values for our simulations.

The bottom panel of Fig. 1 shows the temperature gradients as a function of length of the simulation cell for three different interfacial solid/liquid bond strengths. The temperature profiles for $\varepsilon_{\text{s-l}} = 0.0335$ eV and $\varepsilon_{\text{s-l}} = 0.0798$ eV are shifted by 20 K and 40 K, respectively. The heat source is added at the middle of the solid region and the steady-state temperature profiles show that the gradient in the liquid region is much greater than the solid region, signifying a lower thermal conductivity of the liquid, as expected. Figure 2 shows the Kapitza conductance ($h_K = q/\Delta T$) as a function of the solid/liquid interfacial bond energy parameter. Similar to results from earlier studies,[13,35] h_K follows a power law dependence with increasing interfacial bond. Note, decreasing the steady heat flux drastically (by ~70%) did not change the calculated Kapitza conductance values.

To study the mechanism behind the increase in h_K, we calculate the local phonon DOS of the monolayers of solid atoms immediately adjacent to the interface and in the bulk

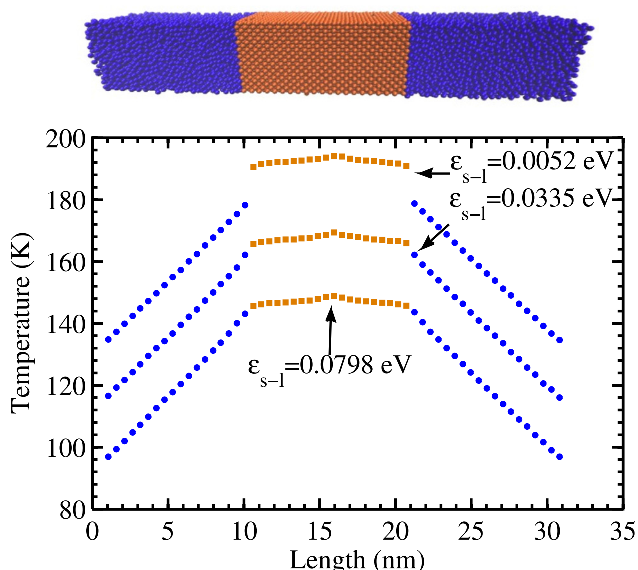

FIG. 1. Top panel: a snapshot of solid/liquid model structure. The orange atoms represent the solid system and the blue atoms represent the liquid system. Bottom panel: the temperature response of the Lennard-Jones systems for three varying interfacial bond strengths under steady state heat flux. The temperature jump at the interface is higher for weak interfacial bonding mimicking poorly wetted solid/liquid interfaces.

This article is copyrighted as indicated in the article. Reuse of AIP content is subject to the terms at: http://scitation.aip.org/termsconditions. Downloaded to IP: 137.54.21.74 On: Tue, 22 Jul 2014 15:57:16

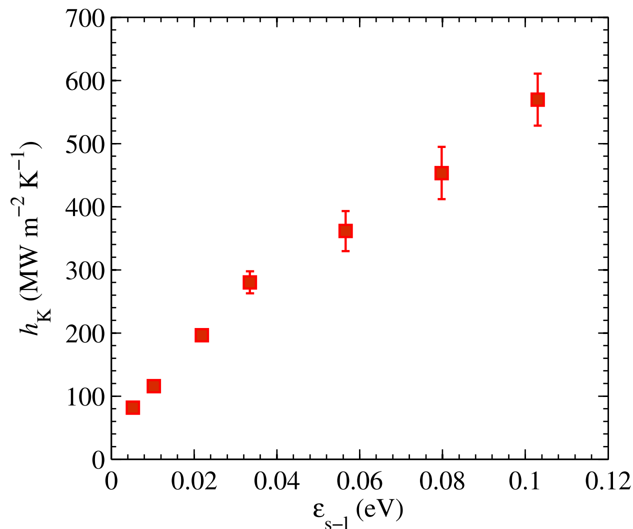

FIG. 2. Thermal boundary conductance as a function of the energy parameter $\varepsilon_{s\text{-}l}$, which defines the strength of the solid/liquid bond.

of the solid. The velocities of the atoms in the monolayers are output every 10 time steps for 300 000 time steps. A velocity autocorrelation function algorithm is used to obtain the local phonon DOS for the monolayers. The details of the process for calculating the DOS are given in Ref. 36.

Figure 3 shows the results of the calculations for different solid/liquid interaction along with the DOS in the "bulk" of the solid, which is not affected by the liquid interaction energies. The results for the poorly wetted, non-interacting surface are expected to be different than the confined or the well wetted, strongly bonded surfaces. In the limit of the most weakly interacting surface, the density of the transverse modes at the interface is roughly the same as those in the bulk, yet shifted towards lower frequency as $\varepsilon_{s\text{-}l}$ is decreased; this is expected for a non-interacting free 2D surface. However, when the bonds between the solid and liquid are strengthened, the peak in the DOS of the solid interfacial atoms associated with the low frequency phonon modes are diminished. For the strongest solid-liquid bond ($\varepsilon_{s\text{-}l} = 0.103$ eV), phonon modes in the 2–3 THz range are noticeably reduced compared to weakest bond ($\varepsilon_{s\text{-}l} = 0.0052$ eV).

From Fig. 3, we can interpret which phonon modes from the solid side enhance thermal transport by transmitting into the liquid region. Comparing the densities of states of various interfacial surfaces with different $\varepsilon_{s\text{-}l}$ lends insight into which modes couple their energy to the adjacent liquid. If there is a channel of energy transport that couples the phonon energy in the solid to that in the liquid, then the energy associated with those phonon modes will be distributed in the solid and liquid regions. Therefore, we would observe a decrease in the DOS at those frequencies in the interfacial monolayer of atoms on the solid. However, if that channel of energy transport does not exist, implying a weaker interaction between the solid and the liquid, phonon modes will not have coupled from the solid to the liquid and the DOS of the interfacial monolayer will appear as a free surface. In line with this argument, the gradual reduction in the DOS of the low frequency phonon mode peak as $\varepsilon_{s\text{-}l}$ is increased (Fig. 3) supports the conclusion that low frequency vibrational energies are coupled to the liquid for the stronger interfacial bonds resulting in higher h_K values (Figs. 1 and 2), whereas the weaker bonds cause the solid monolayer to act as a free surface that does not as readily couple vibrations to the liquid. This spectral shift in phonon energy coupling defines the fundamental thermal mechanisms driving thermal conductance across variably bonded solid/liquid interfaces.

To shed more light into which phonon modes dominate thermal transport, we have separated the local phonon DOS into in-plane and out-of-plane components for the weakest and strongest bonded conditions in Fig. 4. Both the in-plane and out-of-plane DOS in the solid monolayer at the interface become more spectrally broad as ϵ_{s-l} is increased. The majority of the spectral contribution to the solid monolayer DOS in the weakly bonded case comes from the in-plane modes, with only a relatively narrow spectral contribution from the out-of-plane modes. This implies the majority of

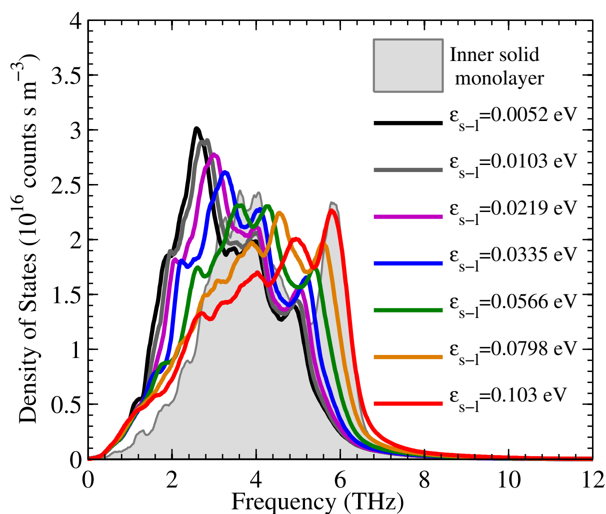

FIG. 3. Local phonon density of states calculated for solid monolayers adjacent to the interface (solid lines) compared to the bulk monolayer (shaded region). Strengthening the interfacial solid/liquid bond softens the low frequency transverse mode in the solid monolayer.

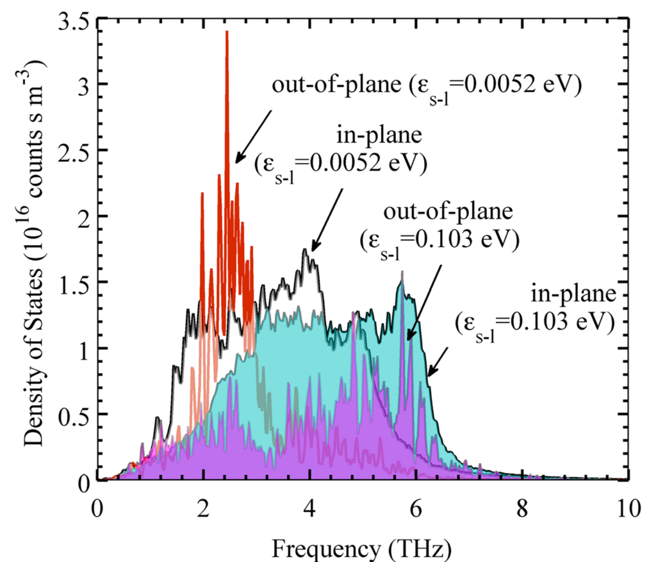

FIG. 4. Local phonon density of states calculated for in-plane and out-of-plane vibrations for weakly ($\varepsilon_{s\text{-}l} = 0.0052$ eV) and strongly ($\varepsilon_{s\text{-}l} = 0.103$ eV) interacting solid/liquid interfaces.

This article is copyrighted as indicated in the article. Reuse of AIP content is subject to the terms at: http://scitation.aip.org/termsconditions. Downloaded to IP: 137.54.21.74 On: Tue, 22 Jul 2014 15:57:16

the frequencies affected by weak bonds at non-wetted solid/liquid interfaces are contained in the in-plane vibrations. Furthermore, comparing the strongly bonded interface to the weakly bonded case, the low frequency DOS diminishes greatly in the solid monolayer for both in-plane and out-of-plane vibrations as $\varepsilon_{s\text{-}l}$ is increased, signifying that low frequency vibrational energies in the solid are primarily affected by variable bonding at the solid/liquid interface. In addition, the spectral breadth, magnitude, and changes in the DOS of the in-plane modes with different bonding conditions signify the direct and important role that transverse modes have on solid/liquid thermal boundary conductance, as we have previously theorized.[22] It is also important to note that higher frequency modes appear in both in- and out-of-plane vibrations upon interfacial stiffening, which is directly correlated to an increase in allowable vibrations due to the increased strength at the solid/liquid interface. Similar to our previous work on bonding effects on solid/solid interfaces,[37] the decrease in bond strength at the solid/liquid interface leads to mode softening of the DOS in the solid, which we observe in both in- and out-of-plane vibrations.

The vibrational spectra of the interfacial solid monolayer can give further insight into the mechanisms of thermal transport by means of a spectrally resolved temperature, T(*f*), where *f* is frequency of the vibrational modes.[38–40] The knowledge of T(*f*) quantitatively defines the strength of vibrational coupling through the interface between two bodies that are characterized by different local temperatures.[37] In order to calculate T(*f*), we must first determine the energy spectrum, $g(f)$ of the solid interfacial monolayer both in equilibrium (eq) and nonequilibrium (NE) conditions. The temperature of the modes is then given as, $T(f) = T_{eq} g_{NE}(f)/g_{eq}(f)$,[38–40] where T_{eq} is the temperature at equilibrium.

Figure 5 shows the spectral temperatures for in-plane (Fig. 5(a)) and out-of-plane (Fig. 5(b)) vibrations of the solid interfacial monolayers with two different wetting conditions.

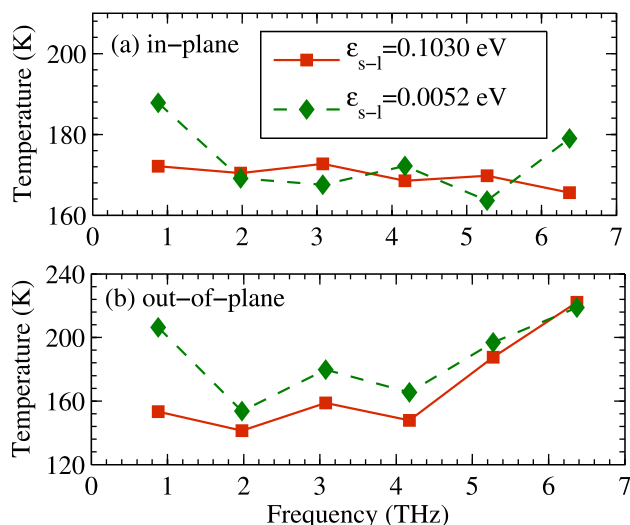

FIG. 5. Spectral temperature, T(*f*), for the (a) in-plane and (b) out-of-plane vibrations of the solid monolayer immediately adjacent to the liquid for two different solid/liquid interfacial bond strengths at an average temperature of 170 K. T(*f*) defines the strength of vibrational coupling through the interface between two bodies that are characterized by different local temperatures.

For the in-plane vibrations, the temperatures of all modes for the strongly bonded case are closer to the equilibrium temperature, suggesting that all the modes are well coupled to the liquid side. For the poorly bonded case ($\varepsilon_{s\text{-}l} = 0.0052$ eV), the temperature of the low frequency modes ($f < 2$ THz) are comparatively higher indicating that low frequency modes are most affected by the solid/liquid interaction. Furthermore, the majority of the phonon modes for the weakly bonded case exist in the 2–5 THz regime (Fig. 4), therefore thermal transport at these interfaces will be dominated by these frequencies; the spectral temperature is lowest for these modes. Similarly, referring to the out-of-plane vibrations, the low frequency spectral temperatures are most affected by the change in bonding. This spectral temperature analysis suggests that low frequency modes augment thermal transport as the interfacial bonding is strengthened.

In conclusion, we show that the increase in thermal boundary conductance across strongly bonded solid/liquid interfaces compared to weakly bonded interfaces is due to increased coupling of low-frequency modes when the solid is better wetted by the liquid. Local phonon density of states and spectral temperature calculations confirm this finding. Specifically, we show that highly wetted solids couple low frequency phonon energies more efficiently, where the interface of a poorly wetted solid acts like free surfaces. Spectral-temperature analysis suggests that low frequency phonon modes are better coupled with stronger solid/liquid interfaces. These observations lend further insight into the experimental and MD studies that have investigated the role of interface conditions on Kapitza conductance across solid/liquid interfaces.

We appreciate support from the Office of Naval research Young Investigator Program (N00014-13-4-0528).

[1]D. G. Cahill, W. K. Ford, K. E. Goodson, G. D. Mahan, A. Majumdar, H. J. Maris, R. Merlin, and S. R. Phillpot, J. Appl. Phys. **93**, 793 (2003).
[2]P. E. Hopkins, ISRN Mech. Eng. **2013**, 682586 (2013).
[3]E. Pop, Nano Res. **3**, 147 (2010).
[4]Z. S. Derewenda and P. G. Vekilov, Acta Crystallogr., Sect. D **62**, 116 (2006).
[5]L. Wang and J. Fan, Nanoscale Res. Lett. **5**, 1241 (2010).
[6]P. Keblinski, S. Phillpot, S. Choi, and J. Eastman, Int. J. Heat Mass Transfer **45**, 855 (2002).
[7]P. Sachdeva and R. Kumar, Appl. Phys. Lett. **95**, 223105 (2009).
[8]P. L. Kapitza, J. Phys. USSR **4**, 181–210 (1941).
[9]H. Harikrishna, W. A. Ducker, and S. T. Huxtable, Appl. Phys. Lett. **102**, 251606 (2013).
[10]Z. Ge, D. G. Cahill, and P. V. Braun, Phys. Rev. Lett. **96**, 186101 (2006).
[11]J. Park, J. Huang, W. Wang, C. J. Murphy, and D. G. Cahill, J. Phys. Chem. C **116**, 26335 (2012).
[12]J.-L. Barrat and F. Chiaruttini, Mol. Phys. **101**, 1605 (2003).
[13]L. Xue, P. Keblinski, S. R. Phillpot, S. U.-S. Choi, and J. A. Eastman, J. Chem. Phys. **118**, 337 (2003).
[14]N. Shenogina, R. Godawat, P. Keblinski, and S. Garde, Phys. Rev. Lett. **102**, 156101 (2009).
[15]H. Acharya, N. J. Mozdzierz, P. Keblinski, and S. Garde, Ind. Eng. Chem. Res. **51**, 1767 (2012).
[16]K. M. Issa and A. A. Mohamad, Phys. Rev. E **85**, 031602 (2012).
[17]B. H. Kim, A. Beskok, and T. Cagin, J. Chem. Phys. **129**, 174701 (2008).
[18]B. Kim, A. Beskok, and T. Cagin, Microfluid. Nanofluid. **5**, 551 (2008).
[19]Z. Shi, M. Barisik, and A. Beskok, Int. J. Therm. Sci. **59**, 29 (2012).
[20]M. Barisik and A. Beskok, Int. J. Therm. Sci. **77**, 47 (2014).
[21]E. T. Swartz and R. O. Pohl, Rev. Mod. Phys. **61**, 605 (1989).
[22]M. E. Caplan, A. Giri, and P. E. Hopkins, J. Chem. Phys. **140**, 154701 (2014).
[23]L. Bocquet and J.-L. Barrat, Soft Matter **3**, 685 (2007).

This article is copyrighted as indicated in the article. Reuse of AIP content is subject to the terms at: http://scitation.aip.org/termsconditions. Downloaded to IP: 137.54.21.74 On: Tue, 22 Jul 2014 15:57:16

[24]J.-L. Barrat and L. Bocquet, Phys. Rev. Lett. **82**, 4671 (1999).
[25]C. Sendner, D. Horinek, L. Bocquet, and R. R. Netz, Langmuir **25**, 10768 (2009).
[26]T. Ohara and D. Torii, J. Chem. Phys. **122**, 214717 (2005).
[27]D. Torii, T. Ohara, and K. Ishida, J. Heat Transfer **132**, 012402 (2009).
[28]D. Bolmatov and K. Trachenko, Phys. Rev. B **84**, 054106 (2011).
[29]D. Bolmatov, V. V. Brazhkin, and K. Trachenko, Sci. Rep. **2**, 421 (2012).
[30]K. Trachenko, Phys. Rev. B **78**, 104201 (2008).
[31]D. V. Matyushov and R. Schmid, J. Chem. Phys. **104**, 8627 (1996).
[32]R. J. Stevens, L. V. Zhigilei, and P. M. Norris, Int. J. Heat Mass Transfer **50**, 3977 (2007).
[33]W. G. Hoover, Phys. Rev. A **31**, 1695 (1985).
[34]F. Muller-Plathe, J. Chem. Phys. **106**, 6082 (1997).
[35]Y. Wang and P. Keblinski, Appl. Phys. Lett. **99**, 073112 (2011).
[36]J. C. Duda, T. S. English, E. S. Piekos, W. A. Soffa, L. V. Zhigilei, and P. E. Hopkins, Phys. Rev. B **84**, 193301 (2011).
[37]J. C. Duda, P. M. Norris, and P. E. Hopkins, J. Heat Transfer **133**, 074501 (2011).
[38]C. F. Carlborg, J. Shiomi, and S. Maruyama, Phys. Rev. B **78**, 205406 (2008).
[39]M. Hu, J. V. Goicochea, B. Michel, and D. Poulikakos, Nano Lett. **10**, 279 (2010).
[40]N. Shenogina, P. Keblinski, and S. Garde, J. Chem. Phys. **129**, 155105 (2008).

This article is copyrighted as indicated in the article. Reuse of AIP content is subject to the terms at: http://scitation.aip.org/termsconditions. Downloaded to IP: 137.54.21.74 On: Tue, 22 Jul 2014 15:57:16